



This open access document is published as a preprint in the Beilstein Archives with doi: 10.3762/bxiv.2019.117.v1 and is considered to be an early communication for feedback before peer review. Before citing this document, please check if a final, peer-reviewed version has been published in the Beilstein Journal of Nanotechnology.

This document is not formatted, has not undergone copyediting or typesetting, and may contain errors, unsubstantiated scientific claims or preliminary data.

**Preprint Title** Comparison of the Effect of Polypyrimidine on Catalytic Performance of Polypyrimidine/CNT as Fuel Cell Catalyst Carrier

**Authors** Naziermu Dongmulati, Caijin Shi and Xieraili Maimaitiyiming

**Publication Date** 07 Okt 2019

**Article Type** Full Research Paper

**Supporting Information File 1** Supplementary Material.doc; 2.9 MB

**ORCID® IDs** Xieraili Maimaitiyiming - <https://orcid.org/0000-0003-1675-5259>

# Comparison of the Effect of Polypyrimidine on Catalytic Performance of Polypyrimidine/CNT as Fuel Cell Catalyst Carrier

Naziermu Dongmulati, Caijin Shi, Xieraili Maimaitiyiming\*

*Key Laboratory of Energy Materials Chemistry, Ministry of Education; Key Laboratory of Advanced Functional Materials, Autonomous Region; Institute of Applied Chemistry, Key Laboratory of Oil and Gas Fine Chemicals, Educational Ministry of China, College of Chemistry and Chemical Engineering, Xinjiang University, Urumqi, 830046 Xinjiang, P. R. China.*

**Abstract:** A new type  $\pi$ -conjugated poly(2,5-didodecyloxy-1,4-diethynyl-phenylene-alt-2-methyl-4,6-pyrimidine) was prepared by Sonogashira polycondensation. A fuel cell catalyst is prepared by depositing platinum particles on carbon nanotubes which was modified with poly(2,5-didodecyloxy-1,4-diethynyl-phenylene-alt-2-methyl-4,6-pyrimidine) and the previously reported poly(2,5-didodecyloxy-1,4-diethynyl-phenylene-alt-2-amino-4,6-pyrimidine). After comparing the two catalysts, it is found that active sites and catalytic performance of catalysts are significantly influenced by the copolymer on the carbon nanotubes which was the catalysis carrier. The electrochemically active surface area (ECSA) of catalysts containing poly(2,5-didodecyloxy-1,4-diethynyl-phenylene-alt-2-methyl-4,6-pyrimidine) was calculated to be  $25.5 \text{ m}^2 \text{ g}^{-1}$ , which is higher than the ECSA of the poly(2,5-didodecyloxy-1,4-diethynyl-phenylene-alt-2-amino-4,6-pyrimidine) containing catalyst ( $18.2 \text{ m}^2 \text{ g}^{-1}$ ). And the first polymer provides better methanol oxidizability and durability than second polymer for catalyst.

**Keywords:** Polypyrimidine; CNTs; Catalyst; Active site

## Introduction

With the increasing demand for energy, the basic research on methanol oxidation is becoming more and more mature (Gong et al. 2018; Liu et al. 2006; WASMUS and KÜVER 1999). In the past few decades, researchers have considered platinum (Pt) to be the most effective catalyst in methanol fuel cell systems (DMFCs)(Sharma et al. 2017; Tiwari et al. 2013; Su et al. 2005). There are many factors affecting the electrocatalytic activity of platinum particles. In order to achieve high activity, stability and high utilization of the catalysts, researchers are vigorously developing suitable catalyst carriers (Lu et al. 2013; Hasche et al. 2010; Tao et al. 2015). Nanocomposites offer new possibilities in this field (Hsu and Chen 2009; Lopez-Bezanilla 2013). The preparation of DMFC catalysts by using the composite materials of conductive polymers and high specific surface area carbon materials as carriers is an effective way to achieve high performance of the catalyst (Okamoto et al. 2009; Muneendra Prasad et al. 2012; Zelikman et al. 2009; Zelikman et al. 2008; Liao et al. 2011; Yameen et al. 2013).

Recent studies have shown that new materials prepared by carbon nanotubes (CNTs) compounded with polymers have new mechanical, electrical, magnetic, optical and chemical properties due to their unique properties (Dongmulati et al. 2018; Sun et al. 2002; Daping et al. 2011). The introduction of the conductive polymer into the electrocatalyst not only helps to improve the dispersibility of the CNTs but also contributes to an improvement in the interface properties between the electrode and the electrolyte. Composites in which the electropolymer and CNTs are combined exhibit the characteristics of a single component having a synergistic effect. However, there have been no reports so far on the influence of polymer structure and specific functional groups on the performance of the catalyst.

We synthesized poly(2,5-didodecyloxy-1,4-diethynyl-phenylene-alt-2-methyl-4,6-pyrimidine) (P1) here, and then used P1 and previously reported poly(2,5-didodecyloxy-1,4-diethynyl-phenylene-alt-2-amino-4,6-pyrimidine)

(P2)(Mamtimin et al. 2010) to modify single-walled carbon nanotubes to prepare P1/CNT and P2/CNT composites as catalyst carriers. After platinum particles (Pt) were deposited on the two complexes to prepare P1/CNT-Pt and P2/CNT-Pt catalysts, we found that the catalysts coated with P1 exhibits higher catalytic activity and better stability than those coated with P2 carbon nanotubes.

## Materials and Methods

All the chemicals used were of analytical grade. 2-amino-4,6-dichloro pyrimidine, 2-methyle-4,6-dichloro pyrimidine,  $(\text{PPh}_3)_4\text{Pd}$ , CuI, Tetrahydrofuran (THF) were purchased from ACROS(China) Chemical Co. and used as received. 1,4-diethynyl-2,5-dodecyloxybenzene were synthesized according to the literature (Mamtimin et al. 2010). The acetonitrile and diisopropylamine were distilled from KOH and toluene was dried and distilled from metal sodium powder under a  $\text{N}_2$  atmosphere. Purified grade Hipco SWCNTs was purchased from XFNANO Materials Tech Co, Ltd and used without any further treatment.

### Synthesis of copolymers

The synthesis method of P1 and P2 is same with each other and following is the typical synthesis method of P1:

2-methyle-4,6-dichloro pyrimidine (0.081 mmol, 13.28 mg) and 1,4-diethynyl-2,5-dodecyloxybenzene (0.081 mmol, 40.08 mg) were added into the 3.5 mL toluene and 1.5 mL diisopropylamine under argon. Then the  $(\text{PPh}_3)_4\text{Pd}$  (0.0039 mmol, 4.5 mg) added to the mixture after protecting by argon for 15 min and reacted at 80 °C for 24 h. After the reaction solution was cooled to room temperature, it was dissolved in 100 mL of dichloromethane, concentrated, and then recrystallized from methanol. After drying overnight at 40 °C, copolymer was isolated in 92% yield.

P1:  $^1\text{H}$  NMR ( $\text{CDCl}_3$ ) d: 7.08–7.10 (m, 2H), 6.82–6.99 (br, 1H), 2.77 (s, 3H) 3.98–4.01 (br, m, 4H), 1.20–1.84 (m, 40H), 0.86 (t, 6H) (S1, S2).

P2:  $^1\text{H}$  NMR ( $\text{CDCl}_3$ ) d: 7.06–7.088 (m, 2H), 6.82–6.99 (br, 1H), 5.18–5.24 (br, d, 2H), 3.98–4.01 (br, m, 4H), 1.20–1.85 (m, 40H), 0.86 (t, 6H) (S3, S4).

### Preparation of composite

The hybrid was prepared by our previous work (Baikeri and Maimaitiyiming 2017). In details: 30 mg of polymer was dissolved in 20 ml of THF, 10 mg of Hipco SCNT was added to the polymer solution and sonicated for 2 h. The mixture was filtered and wash with THF to remove additional polymer. Then, the composites were dried under vacuum for 12 hours to obtain P1/CNT and P2/CNT hybrids.

### **Preparation of catalysts**

The loading of the Pt nanoparticles on the P1/CNT and P2/CNT hybrids was carried out by the reduction of  $\text{H}_2\text{PtCl}_6 \cdot 6\text{H}_2\text{O}$  in an ethylene glycol aqueous solution. First, THF (10 mL) were added to P1/CNT hybrids (10 mg) and sonicated for 1 h, then ethylene glycol (9.9 mL) was added and sonicated for 20 min. Deionized water (6.6 mL) and ethylene glycol (33 mL) aqueous solution of  $\text{H}_2\text{PtCl}_6 \cdot 6\text{H}_2\text{O}$  (0.02388 g) were added to P1/CNT hybrids. The mixture refluxed at 140 °C for 8 h after stirring for 4 h at room temperature. The solid materials was collected by filtration and washed with ethanol, then dried under vacuum to obtain P1/CNT-Pt. Pt was deposited on the surface of the composite in the same manner as preparation of P1/CNT-Pt described above to obtain P2/CNT-Pt catalyst.

### **Preparation of composite electrode**

We prepared the electrolyte solution and protect it with argon for 15 min to remove oxygen and water from the electrolyte solution. The test substance was completely dispersed in THF solvent, and uniformly dripped the solution on a glassy carbon electrode (0.48 mg mL<sup>-1</sup>, 3.0 mm in diameter ) and dried it at room temperature for 20 min. After drying, the electrode was subjected to cyclic voltammetry test with CHI660c electrochemical work station in 1M  $\text{H}_2\text{SO}_4$  solution and 0.5 M  $\text{H}_2\text{SO}_4$  + 0.5 M  $\text{CH}_3\text{OH}$  solution. The working electrode was glassy carbon electrode with an area of 0.07 cm<sup>2</sup>. The electrode is platinum wire electrode, the reference electrode is calomel electrode and the scanning range is -0.13 V to 1 V. The experiments were carried out under argon (25 °C) .

### **Characterization**

Transmission electron microscope (TEM) analysis was done in JEM - 2600F

transmission electron microscope. Thermogravimetric analysis (TGA) was carried out on Germany NETZSCH STA 449F3 thermogravimetric analyzer, in the air heated catalysts from 35 °C to 800 °C with a temperature gradient of 10 °C / min. Ultrasonication was carried out in a KQ5200B bath sonicator (KUN SHAN JIANG SU, CHINA). The cyclic voltammetry (CV) were carried out in a CHI660C type electrochemical workstation with the potential range of -0.13 ~ 1 V and scanning rate of 50 mV / s. Infrared spectroscopy test was done in the German Bruker Spectrometer BRUKER EQUINOX-55 and the sample for the KBr tablet. ESCALAB 250Xi was used for XPS analysis and D8 ADVANCE was used for XRD analysis.

## Results and Discussion

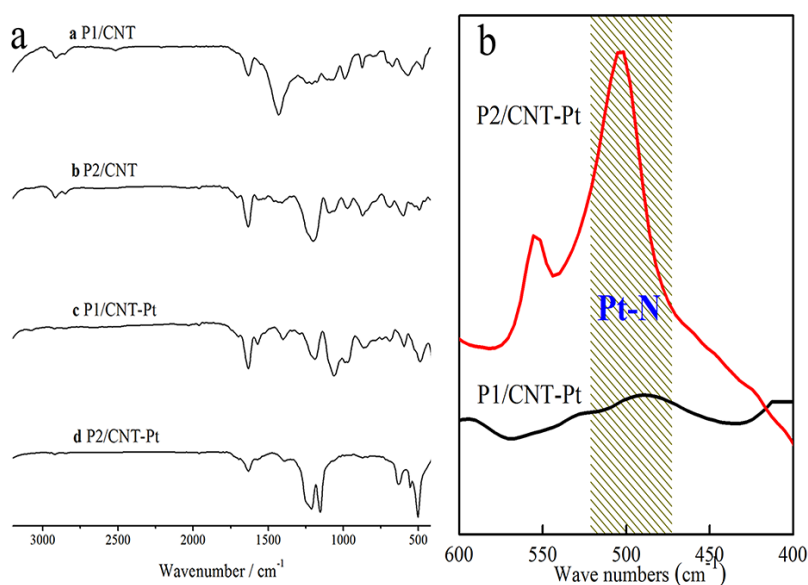


**Figure 1** FT-IR spectrum of P1/CNT, P2/CNT, P1/CNT-Pt and P2/CNT-Pt (a), FT-IR spectrum of P1/CNT-Pt and P2/CNT-Pt (b)

In order to confirm the successful preparation of the catalyst, FT-IR analysis was performed. In Fig.1a, the characteristic peaks of C = N appear at 1620 cm<sup>-1</sup> (a), 1632 cm<sup>-1</sup> (b) and 1635 cm<sup>-1</sup> (c) and 1632 cm<sup>-1</sup> (d), respectively. The skeleton characteristic absorption peak of the aromatic ring can also be detected at 1431 cm<sup>-1</sup> (a), 1417 cm<sup>-1</sup> (b), 1403 cm<sup>-1</sup> (c) 1398 cm<sup>-1</sup> (d). In the curve a and b, typical stretching vibration of the alkyl group was detected at 2922 cm<sup>-1</sup> and 2921 cm<sup>-1</sup>, and the peaks in the curves c and d became inconspicuous. It can also be seen from the figure that all characteristic peaks of the composites P1/CNT (a) and P2/CNT (b) appear in the

spectra of P1/CNT-Pt (c) and P2/CNT-Pt (d). This indicates that platinum particles deposited on this polymer-based carbon nanotubes successfully.

In Fig. 1b, the Far-IR spectrum of P1/CNT-Pt and P2/CNT-Pt exhibited the Pt-N bond at around  $510\text{ cm}^{-1}$  and  $520\text{ cm}^{-1}$ , respectively, indicating that the complex formation of the polypyrimidine with Pt ion, this is consistent with previous literature reports (Dongmulati et al. 2018). It can be seen from the figure that the coordination of P2 and Pt particles is stronger than the coordination of P1 and Pt. This coordination causes electron transfer phenomenon to change the electronic structure around the metal Pt atom with active sites. The N atom coordinates with the Pt atom, but cannot enter the Pt lattice layer and occupies the active site of Pt. Thus, the methanol molecules or oxygen molecules entering the active site of Pt are reduced, and the catalytic performance is lowered (Yin et al. 2013).

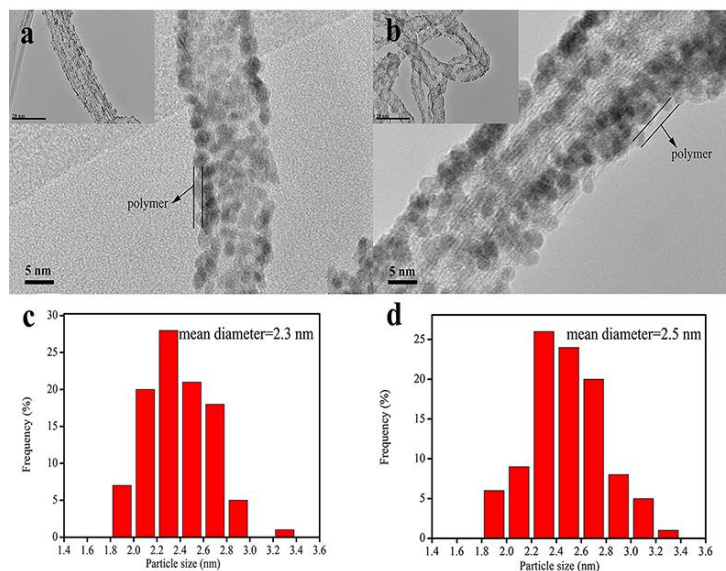


**Figure 2** HRTEM images of P1/CNT-Pt (a) and P2/CNT-Pt (b), Particle size distribution of P1/CNT-Pt (c) and P2/CNT-Pt (d).

We recognized from HRTEM images of the two catalysts depicted in Fig.2 that Pt particles are distributed uniformly on polypyrimidine coated CNTs, the surface of

the CNTs with a tubular structure is uneven because of the coating by polypyrimidine and which is more conducive to the uniform deposition of the platinum nanoparticles. The average particle size and particle size distribution of Pt nanoparticles on P1/CNT and P2/CNT composites were further investigated by counting the particle size of 100 Pt nanoparticles in the TEM image (Fig. 2c and Fig. 2d). It can be seen from Fig. 2a and Fig. 2c that the particle size of Pt nanoparticles on the surface of P1/CNT is mainly distributed among 1.8-3.0 nm and the average particle size is 2.3 nm. Fig. 2b and Fig. 2d are TEM and particle size distribution diagrams of the P2/CNT-Pt catalyst, respectively. For P2/CNT composites, the particle size is mainly distributed among 1.8-3.0 nm with an average particle size of 2.5 nm. The Pt nanoparticles are uniformly dispersed on the surface of the P1/CNT. Comparing Fig. 2 a and 2b, it can be seen that the platinum particles (black spots) accumulated on the surface of the P1/CNT composite are less than that of the P2/CNT, this indicating that P1 can prevent Pt nanoparticles from aggregating with each other, and thus resulting in a uniform dispersion of Pt nanoparticles on the CNTs composite surface. A good dispersion of Pt particles rather than clumping together helps to improve the electrocatalytic activity.

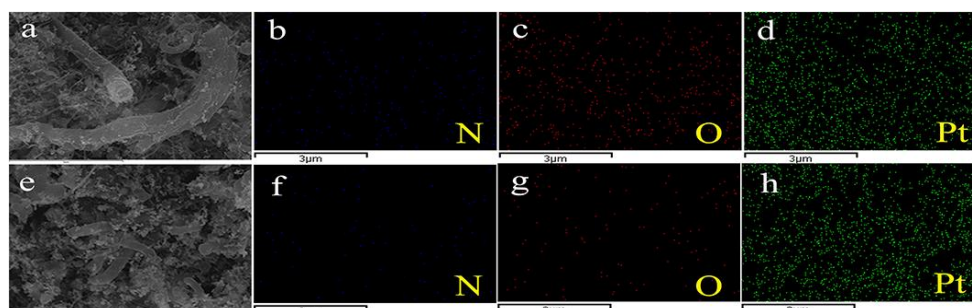


**Figure 3** SEM images of P1/CNT-Pt (a) and P2/CNT-Pt (b), Elemental mapping images of P1/CNT-Pt (b,c,d) and P2/CNT-Pt (f,g,h).

Fig. 3a and 3e show the SEM images of the P1/CNT-Pt and P2/CNT-Pt,

respectively. Fig. 3b-3h present the mapping image of N, O and Pt elements on P1/CNT and P2/CNT hybrids. It can be observed easily from the images that N, O and Pt elements are uniformly distributed on the surface of the CNTs, indicating that the polymers successfully coat the CNTs and  $\text{H}_2\text{PtCl}_6 \cdot 6\text{H}_2\text{O}$  is successfully reduced to Pt particles and deposited on the polymer-based carbon nanotubes. It can also be observed that the N and O elements on P1/CNT-Pt are more than those on P2/CNT-Pt, indicating that P1 is better coated on carbon nanotubes, which provides better electrochemical stability for the catalyst.

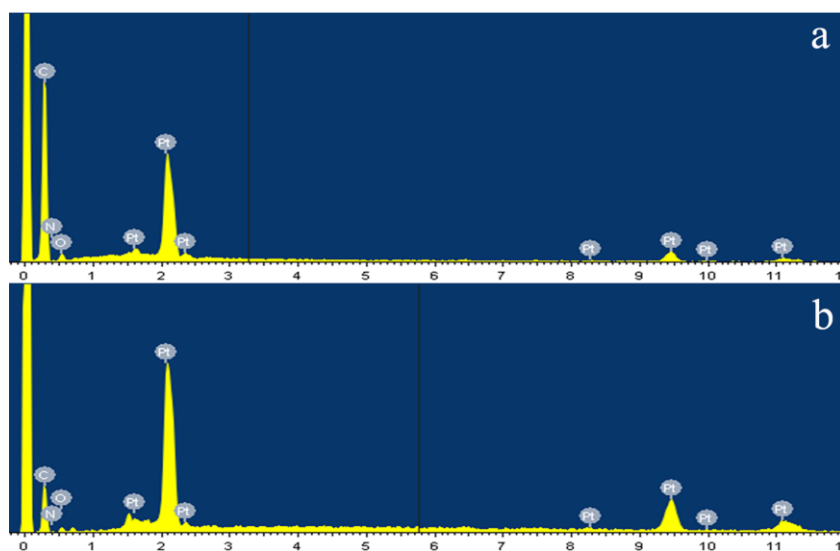


**Figure 4** EDS images of P1/CNT-Pt (a) and P2/CNT-Pt (b).

Fig. 4 shows EDS spectrogram of P1/CNT-Pt (a) and P2/CNT-Pt (b). The N and O elements shown in the figure are derived from P1 and P2. This further demonstrates the successful combination of the polymer with the CNTs. The Pt element is derived from Pt particles reduced by  $\text{H}_2\text{PtCl}_6 \cdot 6\text{H}_2\text{O}$ , which also indicates that Pt are successfully deposited onto the composites.

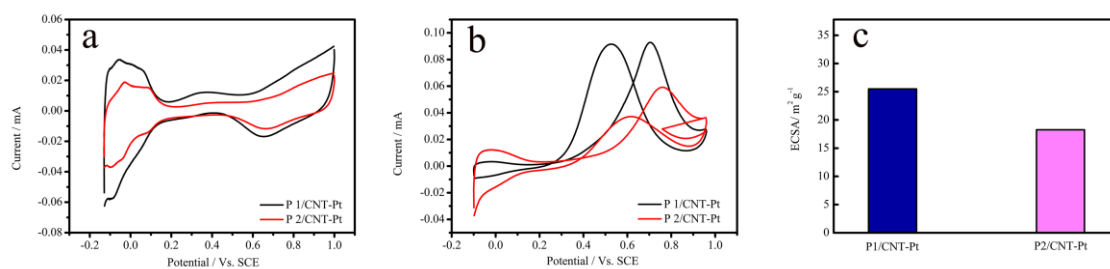


**Figure 5** CV curves of P1/CNT-Pt and P2/CNT-Pt catalysts in 1 M H<sub>2</sub>SO<sub>4</sub> (a), CV curves of P1/CNT-Pt and P2/CNT-Pt catalysts in 0.5 M H<sub>2</sub>SO<sub>4</sub> + 0.5 M CH<sub>3</sub>OH (b), ECSA values of P1/CNT-Pt and P2/CNT-Pt (c).

Fig. 5a shows the cyclic voltammograms (CV) of the P1/CNT-Pt and P2/CNT-Pt catalysts with a scan rate of 50 mV/s in 1 M H<sub>2</sub>SO<sub>4</sub> solution. These catalysts show distinct peaks in the hydrogen adsorption and hydrogen desorption regions. It can be seen from the figure that dehydrogenation peak and double-layer capacitance of P1/CNT-Pt catalyst in 0.1 V-0.4 V is significantly higher than that of P2/CNT-Pt. The electrochemical active surface areas (ECSA) of the catalysts can be calculated by the following equation (1) and listed in the Fig. 5c. It can be seen clearly from the picture that P1/CNT-Pt has the higher ECSA value than P2/CNT-Pt. This is mainly due to the fact that there are fewer active sites on P2/CNT-Pt than on P1/CNT-Pt, which indicates that the catalyst carrier can indeed affect the formation of active sites of Pt, thereby affecting catalytic performance.

$$\text{ECSA} = Q (\text{integral area}) / (\text{sweep speed} \times 2.1 \times \text{concentration} \times \text{volume} \times \text{Pt percentage content}) \quad (1)$$

The electrochemical activity of the catalyst was measured by CV test in 0.5 M H<sub>2</sub>SO<sub>4</sub> + 0.5 M CH<sub>3</sub>OH at room temperature. It can be seen from Fig. 5b that CV curves consisted of two well-defined peaks at the forward and backward scans, which are attributed to the oxidation of methanol molecules at about 0.76 V (vs. SCE) and removal of intermediates at about 0.48 V, respectively (Umeda et al. 2003). It can also be seen that the value of methanol electrooxidation of P1/CNT-Pt is higher than that of P2/CNT-Pt, that is, it has the highest electrocatalytic activity for methanol.

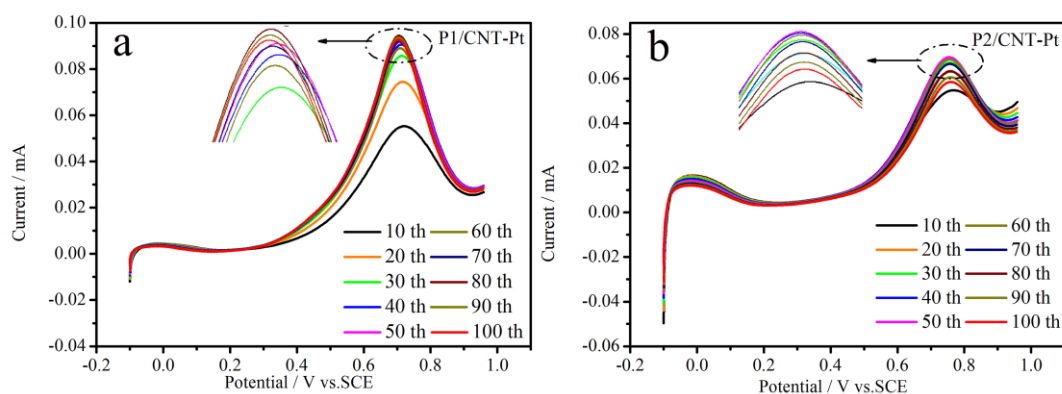


**Figure 6** CV curves of different cycle numbers for P1/CNT-Pt (a) and P2/CNT-Pt (b) in 0.5 M  $\text{H}_2\text{SO}_4+0.5 \text{ M CH}_3\text{OH}$  solution.

In addition to the electroactivity of the catalyst, stability is also an important indicator of the catalyst in commercial applications. Fig. 6a and 6b shows the CVs of different cycle numbers for P1/CNT-Pt and P2/CNT-Pt, respectively. It can be observed that P2/CNT-Pt shift to the positive direction more than P1/CNT-Pt. It can be seen from the enlarged view that the current value of P1/CNT-Pt increases with the number of cycles, and begins to decline at 90 cycles with an unobvious downward trend. However, the current value of P1/CNT-Pt increases slowly with the number of cycles, and starts to decrease significantly after 50 cycles. The current value of 100 cycles for P1/CNT-Pt is similar to that of 10 cycles. In summary, it is obvious that the stability of P2/CNT-Pt is better than that of P1/CNT-Pt.

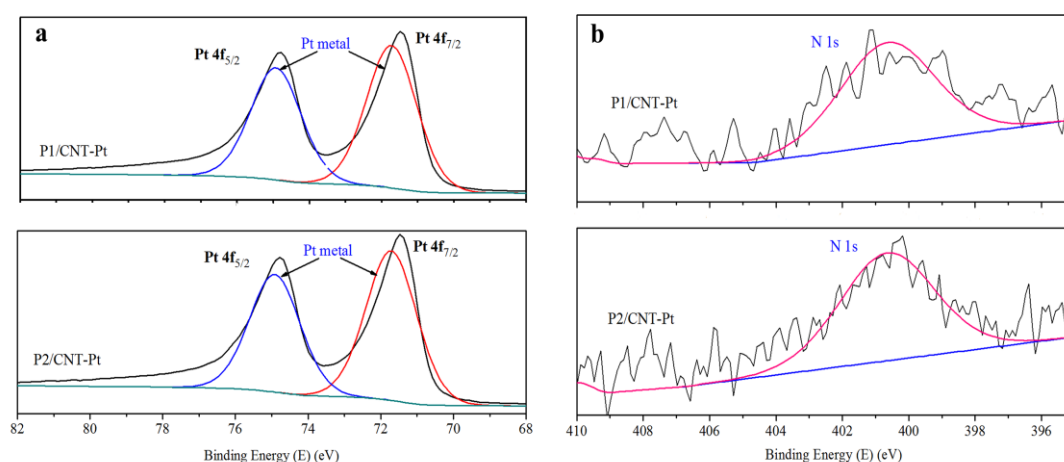


**Figure 7** Pt(4f) bands in P1/CNT-Pt and P2/CNT-Pt (a). N(1s) bands in P1/CNT-Pt and P2/CNT-Pt (b).

The surface composition of the P1/CNT-Pt and P2/CNT-Pt catalysts and the

chemical states of the N and Pt elements were analyzed by XPS spectroscopy. In Fig. 7a, the peak of Pt can be observed, indicating that Pt is adsorbed on the polymer/CNT surface by  $\pi$ - $\pi$  conjugation. The peaks at 400.5 eV (P1/CNT-Pt) and 400.6 eV (P2/CNT-Pt) in the N1s spectrum are attributed to N in the polymer, which also demonstrates that the polymer successfully complexes with CNTs. The polypyrimidine on the surface of the carbon nanotubes facilitates the formation of Pt<sup>0</sup>. Studies have shown that the presence of Pt<sup>0</sup> in the catalyst results in better catalytic performance of the catalyst because Pt<sup>0</sup> provides more active sites than Pt<sup>2+</sup> and Pt<sup>4+</sup> (Han et al. 2014; Yin et al. 2013).

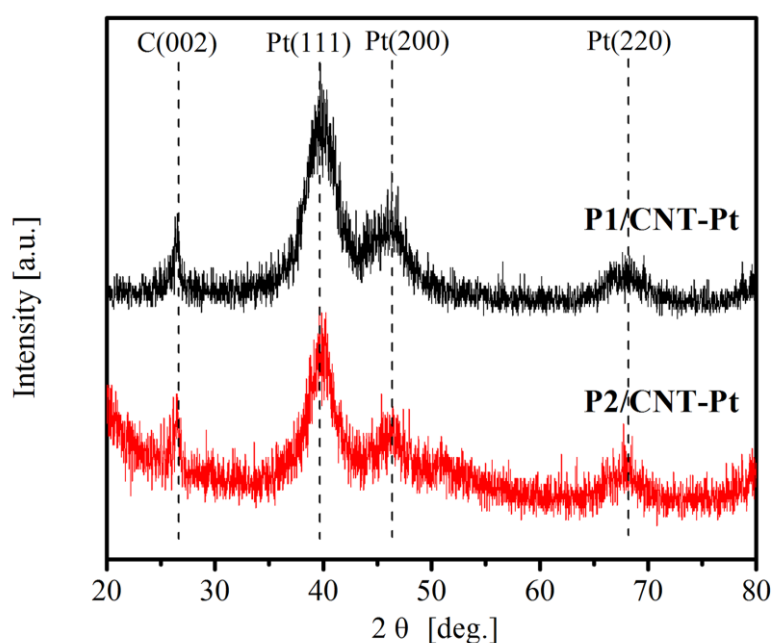


**Figure 8** XRD spectrum P1/CNT-Pt and P2/CNT-Pt.

Fig. 8 is the X-ray diffraction (XRD) spectrum of P1/CNT-Pt and P2/CNT-Pt. The peaks at  $2\theta = 39.65^\circ$ ,  $46.39^\circ$  and  $68.18^\circ$  are corresponding to the (111), (200) and (220) planes of Pt, respectively. The diffraction peak caused by carbon carrier was a peak at  $2\theta = 26.63^\circ$ , indicating that the Pt was successfully supported on carbon nanotubes. The results are consistent with TEM results. It can also be seen from the figure that the characteristic diffraction peaks corresponding to Pt (111), (200) and (220) in curve P1/CNT-Pt are broadened relative to the characteristic diffraction peaks in curve P2/CNT-Pt, indicating that the average size of Pt nanoparticles deposited on

the P1/CNT is smaller than that deposited on the P2/CNT, this is consistent with the particle size distribution results.

## **Conclusions**

In conclusion, fuel cell catalysts are prepared by depositing platinum particles on CNTs which was modified with copolymers, and characterized by SEM, HRTEM, XRD and CV test. After comparing, it is found that active sites and catalytic performance of catalysts are significantly influenced by the copolymer on the carbon nanotubes which was the catalysis carrier. A fuel cell catalyst prepared by modifying CNTs with P1 has higher ECSA value and better methanol oxidizability than the catalyst which was prepared by modifying CNTs with P2.

## **Conflicts of interest**

There are no conflicts to declare.

## **Acknowledgments**

The authors gratefully acknowledge the support from the National Natural Science Foundation of China (no. 21164012, 51763021, 51363020 ).

## **References**

- [1] Baikeri S, Maimaitiyiming X. Polypyrimidine/SWCNTS composite comprising Pt nanoparticles: Possible electrocatalyst for fuel cell[J]. Polymer Science, 2017, 59(5):1-7.
- [2] He D, Chao Z, Cheng X, et al. Polyaniline-Functionalized Carbon Nanotube Supported Platinum Catalysts[J]. Langmuir, 2011, 27(9):5582-5588.
- [3] Dongmulati N, Baikeri S, Maimaitiyiming X, et al. Comparison of different types of polypyrimidine/CNTs/Pt hybrids in fuel cell catalysis[J]. Journal of Nanoparticle Research, 2018, 20(8):210.
- [4] Gong L, Yang Z, Li K, et al. Recent development of methanol electrooxidation catalysts for direct methanol fuel cell[J]. Journal of Energy Chemistry, 2018(6):S2095495617310380.

- [5] Han L, Liu H, Cui P, et al. Alloy Cu<sub>3</sub>Pt nanoframes through the structure evolution in Cu-Pt nanoparticles with a core-shell construction[J]. *Scientific Reports*, 2014, 4(6414):6414.
- [6] Hasché F, Oezaslan M, Strasser P. Activity, stability and degradation of multi walled carbon nanotube (MWCNT) supported Pt fuel cell electrocatalysts[J]. *Physical Chemistry Chemical Physics*, 2010, 12(46):15251-15258.
- [7] Hsu R S, Higgins D, Chen Z. Tin-oxide-coated single-walled carbon nanotube bundles supporting platinum electrocatalysts for direct ethanol fuel cells[J]. *Nanotechnology*, 2010, 21(16):165705.
- [8] Liao Y , Zhang C , Zhang Y , et al. Carbon Nanotube/Polyaniline Composite Nanofibers: Facile Synthesis and Chemosensors[J]. *Nano Letters*, 2011, 11(3):954-959.
- [9] Liu H, Song C, Lei Z, et al. A review of anode catalysis in the direct methanol fuel cell[J]. *Journal of Power Sources*, 2006, 155(2):95-110.
- [10] Lopezbezanilla A. Electronic Transport Properties of Chemically Modified Double-Walled Carbon Nanotubes[J]. *Journal of Physical Chemistry C*, 2013, 117(29):15266–15271.
- [11] Lu J, Hong L, Yang Y, et al. Phosphotungstic acid-assisted preparation of carbon nanotubes-supported uniform Pt and Pt bimetallic nanoparticles, and their enhanced catalytic activity on methanol electro-oxidation[J]. *Journal of Nanoparticle Research*, 2014, 16(1):2162.
- [12] Mamtimin X, Matsidik R, Nurulla I. New soluble rigid rod copolymers comprising alternating 2-amino-pyrimidine and phenylene repeat units: Syntheses, characterization, optical and electrochemical properties[J]. *Polymer*, 2010, 51(2):437-446.
- [13] Prasad A M, Santhosh C, Grace A N. Carbon nanotubes and polyaniline supported Pt nanoparticles for methanol oxidation towards DMFC applications[J]. *Applied Nanoscience*, 2012, 2(4):457-466.
- [14] Okamoto M, Fujigaya T, Nakashima N. Design of an assembly of poly(benzimidazole), carbon nanotubes, and Pt nanoparticles for a fuel-cell electrocatalyst with an ideal interfacial nanostructure.[J]. *Small*, 2010, 5(6):735-740.
- [15] Sharma M , Jung N , Yoo S J . Toward High-Performance Pt-Based Nanocatalysts for Oxygen Reduction Reaction through Organic–Inorganic Hybrid Concepts[J]. *Chemistry of Materials*, 2018, 30(1):2-24.
- [16] Su F, Zeng J, Bao X, et al. Preparation and Characterization of Highly Ordered Graphitic Mesoporous Carbon as a Pt Catalyst Support for Direct Methanol Fuel Cells[J]. *Chemistry of Materials*, 2005, 17(15):3960-3967.

- [17] Sun Y P, Fu K, Lin Y, et al. Functionalized Carbon Nanotubes: Properties and Applications[J]. *Acc Chem Res*, 2002, 35(12):1096-1104.
- [18] Li T, Dou S, Ma Z, et al. Platinum Nanoparticles Supported on Nitrobenzene-Functionalized Multiwalled Carbon Nanotube as Efficient Electrocatalysts for Methanol Oxidation Reaction[J]. *Electrochimica Acta*, 2015, 157:46-53.
- [19] Tiwari J N, Tiwari R N, Singh G, et al. Recent progress in the development of anode and cathode catalysts for direct methanol fuel cells[J]. *Nano Energy*, 2013, 2(5):553-578.
- [20] Umeda M, Kokubo M, Mohamedi M, et al. Porous-microelectrode study on Pt/C catalysts for methanol electrooxidation[J]. *Electrochimica Acta*, 2003, 48(10):1367-1374.
- [21] WASMUS, KÜVER. Methanol oxidation and direct methanol fuel cells : a selective review[J]. *Journal of Electroanalytical Chemistry*, 1999, 461(1-2):14-31.
- [22] Yameen B, Zydziak N, Weidner S M, et al. Conducting Polymer/SWCNTs Modular Hybrid Materials via Diels-Alder Ligation[J]. *Macromolecules*, 2013, 46(7):2606-2615.
- [23] Yin Z, Chi M, Zhu Q, et al. Supported bimetallic PdAu nanoparticles with superior electrocatalytic activity towards methanol oxidation[J]. *Journal of Materials Chemistry A*, 2013, 1(32):9157-9163.
- [24] Zelikman E, Narkis M, Siegmann A, et al. Polyaniline/multiwalled carbon nanotube systems: dispersion of CNT and CNT/PANI interaction.[J]. *Polymer Engineering & Science*, 2010, 48(10):1872-1877.
- [25] Zelikman E, Suckeveriene R Y, Mechrez G, et al. Fabrication of composite polyaniline/CNT nanofibers using an ultrasonically assisted dynamic inverse emulsion polymerization technique[J]. *Polymers for Advanced Technologies*, 2009, 21(2):150-152.